Fundamental Journal of Modern Physics
Vol. 5, Issue 2, 2013, Pages 19-46
Published online at http://www.frdint.com/

PHYSICS OF ELECTROSTATIC RESONANCE WITH NEGATIVE PERMITTIVITY AND IMAGINARY INDEX OF REFRACTION FOR ILLUMINATED PLASMOID IN THE EXPERIMENTAL SET UP FOR MICROWAVE NEAR FIELD APPLICATOR

SHANTANU DAS[1,*], RAJESH KUMAR[2], TITTO JOHN GEORGE[3], AMIT BANSAL[4], NITIN KUMAR LAUTRE[5] and APURBA KUMAR SHARMA[4]

[1]Scientist (H+), & UGC-Visiting Fellow at Dept. Applied Mathematics
University of Calcutta
Reactor Control Division
Bhabha Atomic Research Centre (BARC)
Mumbai-400085
e-mail: shantanu@barc.gov.in

[2]Scientist-G, IADD, FOTIA
Bhabha Atomic Research Centre (BARC), Mumbai

[3]Department of Mechanical Engineering
VJCET, Kerala, India

[4]Department of Mechanical and Industrial Engineering
IIT Roorkee, Roorkee, India

[5]Mechanical Engineering Department
Visvesvarya National Institute of Technology
Nagpur, India

Keywords and phrases: electrostatic resonance, negative permittivity, Fredholm's integral equation, meta-material, surface-plasmon-polariton (SPP), surface waves, imaginary refractive index.
*Corresponding author
Received April 9, 2013

Abstract

In this paper electrodynamics of plasmoid lighting is explained, which we are generating via creation of localized hot spot by application of microwave energy. The microwave radiation is applied via co-axial applicator, the monopole antenna; and the 'near field' of the radiation causes local hot spots and thereby thermal runaway causing ejection of small particles from the base substrate. These particles interact with the Electromagnetic field, and due to electrostatic resonances occurring from negative dielectric permittivity (thereby imaginary refractive index) of these small particles, giant electromagnetic energy fields are locally accumulated; making local discharge thus giving illuminated plasmoid ball. This paper explains the formation of giant electric field at electrostatic resonance, which is primary cause of localized discharge thus plasmoid illumination, is observed in microwave drilling experiments.

Introduction

The natural phenomena of fire-ball usually occur after a lightning strike that may lead to plasma formation and a source of considerable electromagnetic (EM) radiation, this is observed in nature and other experimentalists as reported in [45]-[51], and also in our experiments with near field microwave applicator. If the frequency of this spectrum of EM radiation is such that the di-electric permittivity of the formed plasma is negative (equivalently the refractive index an imaginary value) then electrostatic resonances may occur [45]-[53]. Electrostatic resonances may produce considerable accumulation of EM energy, giving 'giant' local fields, [1]-[10], [14], [19], [27], [29], [35], [38], which may visually manifest as plasmoid lighting [45]-[53]. This is plausible explanation of the 'fire-balls' observed in nature. In our experiment of 'material processing with microwave', we are using a near field co-axial applicator (Figure 1) through a monopole antenna, to an object (bone, cement, concrete, thin copper sheet, thin aluminum sheet, glass etc), in order to melt via dielectric heating and thermal runaway principle; through 'resonating near field' region of monopole. The molten object (which takes about 5-10 second, after application of microwave power of 150-200 Watts radiating at 2.54 GHz) when pierced by the monopole itself in order to drill the object; gets exposed to microwave radiation and absorbs more microwave to form plasma, which behaves exactly as natural fire-ball. The difference is the plasmoid ball in our case carries the original substrate material composites (bone, glass silica, aluminum, copper glass particles) where as the atmospheric fire-ball contains composites of air breakdown. In this paper the detailed physics of electrodynamics aspect of plasmoid lighting is explained, as the particles which comes out from molten substrate behaves as negative epsilon material, accumulating large surface charges (Surface Plasmon Polaritons, SPP), the phenomena of surface plasmon resonances, causes local giant fields, making local discharges [1-10, 14, 19, 27, 29, 35, 38]; causing illumination, i.e., lit plasmoid. Same plasmoid is observed in other experiments as reported in [45-51].

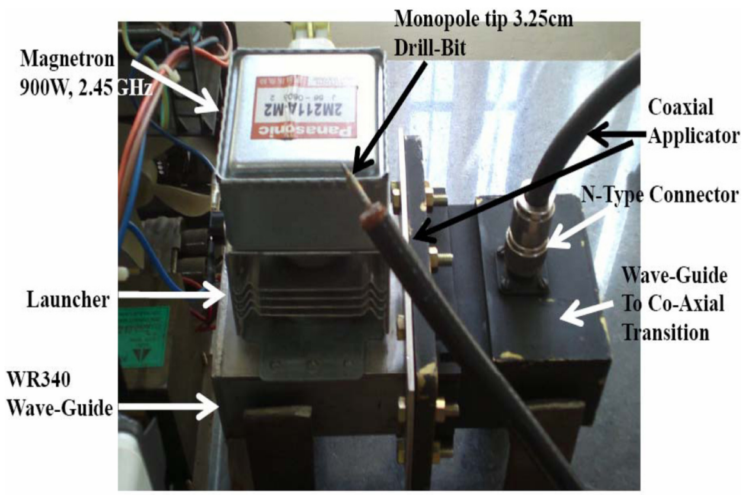

Figure 1. The set up of microwave near field applicator with monopole.

Figure 2 and Figure 3 give the result of drilling of bone and aluminum sheets via co-axial near field applicator. The same has been tried on glass, concrete, cement, wood, and while doing the experiment, illuminated plasmoid formation is observed, depicted in Figures 4a and 4b. The Figure 4a gives picture of co-axial drill bit in open atmosphere, while Figure 4b, gives drilling picture inside electromagnetic EM shielded chamber (microwave oven box).We shall be dealing with electrodynamics aspect of the plasmoid illumination aspect and will give plausible reasoning. Why we are calling the plasmoid [45-51] instead a plasma ball is, due to seemingly lesser number density of sparsely placed particles which accumulated surface charges; as compared to large number density of free charges in the case of real plasma. This plasmoid may be a case of dusty plasma.

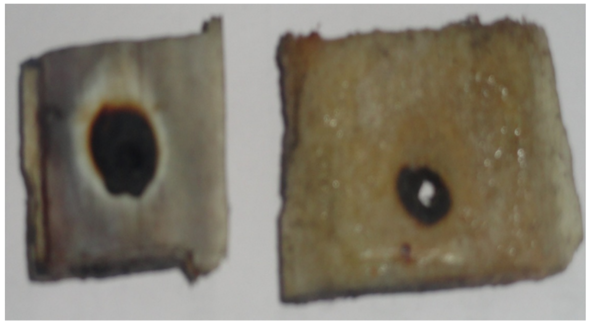

Figure 2. Bone drilled with co-axial applicator near field.

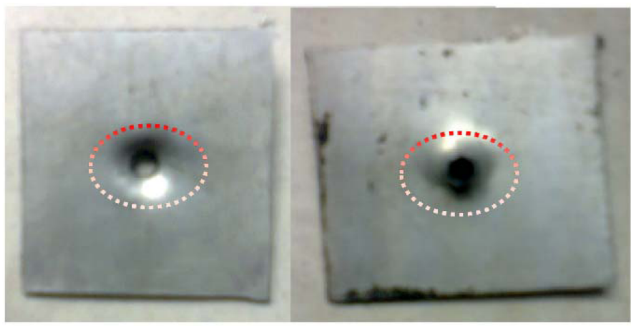

Figure 3. Aluminum plate 0.7mm drilled via near field.

2. Review of Wave Mechanism and Boundary Conditions

In this section we shall be reviewing our concepts of electromagnetic wave propagation and boundary conditions. In doing so we shall be assuming quasi static approximations, for simplification of the derived concepts of surface waves, propagating and bounded conditions, reflection and transmissions at the boundary [1-10, 14, 19, 27, 29, 35, 38].

2.1. Propagating wave

Let an EM radiation (TE or TM) travel in media number-1, from $-\infty < z < 0,$ in $+z$ direction with media properties dielectric permittivity and permeability as $\varepsilon_1, \mu_1;$ encounters a boundary at $z = 0;$ Figure 5. The media number-2 extends from $0 < z < \infty,$ with properties ε_2 and $\mu_2.$ The boundary conditions at the interface $z = 0,$ where t is tangential component, and n is the normal component at the boundary are expressed in (1). The following (1) formulation ignores surface currents and surface charges. The formulation (1) states that tangential components of electric and magnetic field and normal components of electric and magnetic flux densities are continuous at the boundary.

$$H_{1t} = H_{2t}, \quad E_{1t} = E_{2t}, \quad \varepsilon_1 E_{1n} = \varepsilon_2 E_{2n}, \quad \mu_1 H_{1n} = \mu_2 H_{2n}. \tag{1}$$

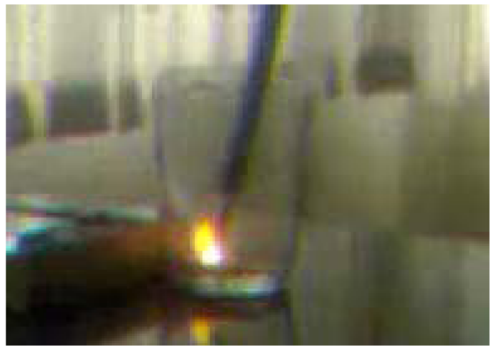

4a. Drilling with co-axial applicator in open atmosphere.

4b. Drilling with co-axial applicator inside EM shielded chamber.

Figure 4. Formation of plasmoid and its illumination.

Let us take a case of TM polarization, the *y*-component of magnetic field is:

$$H_{y1} = Ae^{-i(k_{z1}z+k_{x1}x)} + Be^{i(k_{z1}z-k_{x1}x)} \tag{2}$$

The number A is incident and B is reflected amplitude in medium-1. Refer Figure 5. The imaginary number $i = \sqrt{-1}$; electrical engineers calls it $j = \sqrt{-1}$. The wave vectors satisfy the following condition in the medium-1, [1-10, 14, 19, 27, 29, 35, 38].

$$k_{z1}^2 + k_{x1}^2 = k_1^2 = \omega^2\mu_1\varepsilon_1. \quad (3)$$

Applying Maxwell's curl condition, we get Electric field in medium-1 as:

$$E_{x1} = -\frac{1}{i\omega\varepsilon_1}\frac{\partial}{\partial z}H_{y1} = \frac{k_{z1}}{\omega\varepsilon_1}\left[Ae^{-i(k_{z1}z+k_{x1}x)} - Be^{i(k_{z1}z-k_{x1}x)}\right]. \quad (4)$$

In medium-2 only transmitted component appears with amplitude C, we write Y-component of magnetic field as:

$$H_{y2} = Ce^{-i(k_{z2}z+k_{x2}x)} \quad (5)$$

The curl of which is:

$$E_{x2} = -\frac{1}{i\omega\varepsilon_2}\frac{\partial}{\partial z}H_{y2} = \frac{k_{z2}}{\omega\varepsilon_2}Ce^{-i(k_{z2}z+k_{x2}x)}. \quad (6)$$

At the boundary $z = 0$ matching is possible if the fields vary in the same manner in the x-direction, which is possible if $k_{xl} = k_{x2}$, meaning phase velocity along x-direction must be same on both sides of the boundary. It follows from geometry that $k_{x1} = k_1 \sin\theta_1$, where θ_1 is the incident angle, and $k_{x2} = k_2 \sin\theta_2$, where, θ_2 is angle of refraction, and $k_1 = \omega\sqrt{\varepsilon_1\mu_1}$, $k_2 = \omega\sqrt{\varepsilon_2\mu_2}$ and $\omega = 2\pi f$, the angular temporal frequency, in radian/second. From which we get usual Snell's law that is (7), with $n_{1,2}$ indicating refractive index of the medium, 1 and 2.

$$\omega\sqrt{\mu_1\varepsilon_1}\sin\theta_1 = \omega\sqrt{\mu_2\varepsilon_2}\sin\theta_2, \qquad n = \frac{n_1}{n_2} = \frac{\sin\theta_1}{\sin\theta_2} = \sqrt{\frac{\mu_2\varepsilon_2}{\mu_1\varepsilon_1}}. \quad (7)$$

Further matching conditions, from tangential field components at the boundary are $A + B = C$, from the condition $H_{y1} = H_{y2}$, at $z = 0$, and $(k_{z1}/\varepsilon_1)(A - B) = (k_{z2}/\varepsilon_2)C$ getting from condition $E_{x1} = E_{x2}$ from $z = 0$. Here we can define reflection and transmission coefficients, as $R = B/A$ $= (1 - \zeta_e)/(1 + \zeta_e)$, $T = C/A = 2/(1 + \zeta_e)$ where $\zeta_e \triangleq (\varepsilon_1 k_{z2})/(\varepsilon_2 k_{z1})$. If instead of TM polarization, it were TE polarized wave, then with incident Electric Field in y-direction, then above derivation remains same, but ζ_e, needs be replaced with ζ_m, defined as $\zeta_m \triangleq (\mu_2 k_{z1})/(\mu_1 k_{z2})$ [1-10, 14, 19, 27, 29, 35, 38].

2.2. Bounded wave (eigen-solution resonance)

Let us now explore another aspect of wave mechanics, namely that the wave can stick to the boundary. When it does so it is called the 'surface' wave, [1-10, 14, 19, 27, 29, 35, 38]. Assuming again TM wave as assumed in earlier section, the new feature is that, waves can propagate along the boundary (in our case in the *x*-direction), but their amplitudes decline exponentially away from $(z = 0)$ the boundary, (in the *z*-direction). This is "bounded wave", can happen only if k_x is sufficiently high $(k_x > k)$, so that $k_z = \sqrt{k^2 - k_x^2}$ in media 1, and 2 implying k_{z1}, k_{x2} are imaginary numbers and thus replaced by $-i\kappa_1$, $-i\kappa_2$ where κ_1, κ_1 are real (positive). Hence the propagation coefficient in the *x*-direction is obtained as: ${k_x}^2 = {k_1}^2 + {\kappa_1}^2 = {k_2}^2 + {\kappa_2}^2$. We are looking for a wave that can exist on surface without an input. In more pretentious language we are looking for "eigen-solutions" (resonances). That is in terms of (2) and (5) with input $A = 0$ the components *B*, and *C* exists and are finite numbers; that is amplitude of wave that declines away from boundary in negative *z*-direction, in medium-1 (B); and decays exponentially from the boundary in positive *z*-direction in medium-2, (C) respectively, (without input that is A). This is eigen-solution (resonance), depicted in Figure 5. In terms of meta-materials we call this process as Surface Plasmon Polariton (SPP), SPP-Wave, Surface Resonance, or Surface Plasmon Resonance; [1-10, 14, 19, 27, 29, 35, 38]; Figure 6.

The equation of magnetic and electric field in medium 1 and 2, for the SPP or resonance case is

$$H_{y1} = Be^{\kappa_1 z}e^{-ik_x x}, \qquad H_{y2} = Ce^{-\kappa_2 z}e^{-ik_x x} \tag{8}$$

Apply curl expression to get, electric field in *x*-direction

$$E_{x1} = \frac{-\kappa_1}{i\omega\varepsilon_1}Be^{\kappa_1 z}e^{-ik_x x}, \qquad E_{x2} = \frac{\kappa_2}{i\omega\varepsilon_2}Ce^{-\kappa_2 z}e^{-ik_x x} \tag{9}$$

Apply again curl expressions to get electric field *z*-indirection

$$E_{x1} = \frac{-k_x}{\omega\varepsilon_1}Be^{\kappa_1 z}e^{-ik_x x}, \qquad E_{z2} = \frac{-k_x}{\omega\varepsilon_2}Ce^{-\kappa_2 z}e^{-ik_x x}. \tag{10}$$

2.3. Resonance conditions (eigen-solutions) are satisfied for negative dielectric permittivity and imaginary refractive index

In this section we will derive, that if one of the media is having negative dielectric permittivity, the bounded waves (SPP) appear as surface plasmon resonance. In order to satisfy boundary conditions of the eigen-solution that is bounded wave sticking to the surface, we need to match H_y and E_x at $z = 0$, which gives; $B = C$ thereby we obtain

$$-\frac{\kappa_1}{\varepsilon_1} = \frac{\kappa_2}{\varepsilon_2}. \tag{11}$$

Note that we have taken, κ_1, κ_2 both real positive (previous section). Therefore the condition (11) is satisfied only if; the dielectric permittivity of medium-2 is negative, that is

$$\varepsilon_2 < 0. \tag{12}$$

This is the condition of existence of electric surface waves or electric resonance (or electrostatic resonance). The (12) is also equivalent to having $\zeta_e = -1$ from $\zeta_e = (\varepsilon_1 k_{z2})/(\varepsilon_2 k_{z1})$.

Now we substitute, in $k_x{}^2 = k_1{}^2 + \kappa_1{}^2 = k_2{}^2 + \kappa_2{}^2$, the value of κ_1 and κ_2 above to have relation in k_x and ω, by using the free space expressions, $k_1 = \varepsilon_{r1}\mu_{r1}k_0$, $k_2 = \varepsilon_{r2}\mu_{r2}k_0$, with $\mu_{r1} = \mu_{r2} = 1$ and $k_0 = \omega/c$; to get dispersion of SPP that is $k_x = (\omega/c)\sqrt{(\varepsilon_{r1}\varepsilon_{r2})/(\varepsilon_{r1} + \varepsilon_{r2})}$. The SPP wave is travelling along the boundary surface; and like travelling wave the wave-vector is k_x, in *x*-direction should be real positive (note this is bounded in *z*-direction). With $\varepsilon_{r2} < 0$ we may write

$$\varepsilon_{r1}\varepsilon_{r2} < 0, \qquad \varepsilon_{r1} + \varepsilon_{r2} < 0. \tag{13}$$

The (13) is more general to (12), relative permittivity is used $\varepsilon = \varepsilon_r\varepsilon_0$ and $\mu = \mu_r\mu_0$ with ε_0 and μ_0 are the free space values. Write the negative relative permittivity as $\varepsilon_{r2} = -n^2$, where *n* indicates refractive index (imaginary refractive index). Then in terms of refractive indexe we get, $k_2{}^2 = \mu_{r2}\varepsilon_{r2}k_0^2 = -n^2k_0^2$ gives

$\kappa_1 = \sqrt{k_x^2 - k_0^2}$, and $\kappa_2 = \sqrt{k_x^2 - k_2^2} = \sqrt{k_x^2 + (nk_0)^2}$.

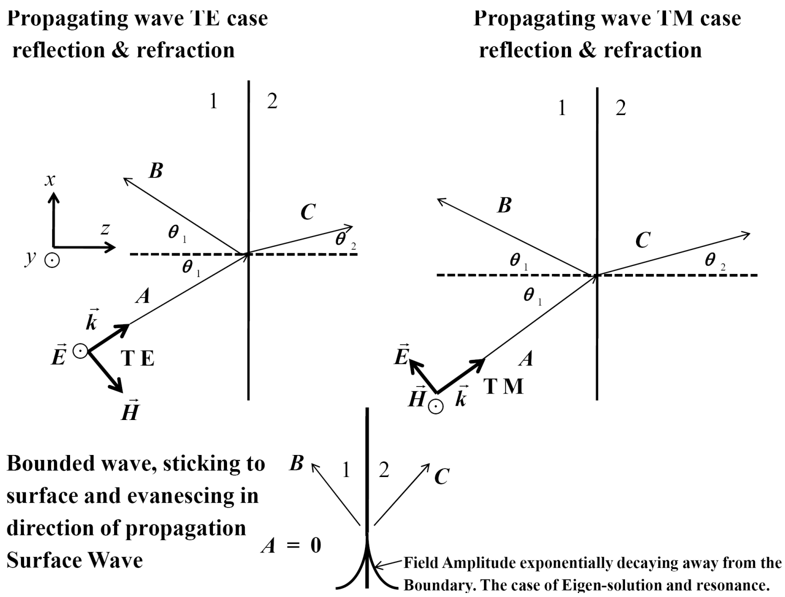

Figure 5. Propagating and surface waves.

3. Appearance of Giant Fiant at Electrostatic Resonance with Negative Sielectric Permittivity and Imaginary Refractive Index

Having seen the basics of surface waves resonance phenomena, in previous section we go further with electrodynamics of imaginary refractive index. Let us consider metal, a flat metal surface is almost a perfect reflector of electromagnetic waves in visible region, and application of metal films as mirrors has a long history. Metal films become 'semi-transparent' at 'resonant' wavelengths (frequencies), allowing the excitation of EM waves propagating on the surface. Consider a thin metal film surface, in the optical and IR spectral ranges the collective excitation of the free electron density coupled to EM fields result in SPP. SPP can be excited when we have negative dielectric permittivity, as described in previous section. The metal film in visible and IR ranges has $\varepsilon_m = \varepsilon'_m - i\varepsilon''_m$, with $\varepsilon'_m < 0$ negative, and loss factor very less $(\varepsilon''_m / \varepsilon'_m) << 1 \sim 0$. Let the medium-1 a free space at $(-\infty < z < \infty)$, with $\varepsilon_{r1} = \mu_{r1} = 1$ and the metal be the medium-2 placed at $z = 0$, and the property for $0 < z < \infty$ is $\varepsilon_{r1} = -n^2 < 0, \mu_{r2} = 1$ (Figure 6) field decaying in z-direction and travelling in $\underline{x}$-direction for a bounded wave (SPP) is

$$H_{y1} = H_0 \exp(ik_x x + k_{z1} z);\ z < 0, \quad H_{y2} = H_0 \exp(ik_x x - k_{z2} z);\ z < 0. \tag{14}$$

The espression in (14) have the SPP wave vector as k_x where $k_{z1} = \sqrt{k_x^2 - k_1^2} = \sqrt{k_x^2 - k_0^2}$ and $k_{z2} = \sqrt{k_x^2 - k_2^2} = \sqrt{k_x^2 - \varepsilon_m k_0^2} = \sqrt{k_x^2 + (nk_0)^2}$, with $k_0 = \omega/c$ as the free space wave vector and $n = \sqrt{-\varepsilon_m} = i\sqrt{\varepsilon_m}$; the imaginary refractive index. The continuity of tangential component of the magnetic field at the boundary $z = 0$, are satisfied as: $H_{y1}(x, z = 0) = H_{y2}(x, z = 0)$. The Electric field is found from Maxwell's curl expression; and are curl $H = -ik\varepsilon E$ with $\varepsilon = 1$ for $z < 0$, and $\varepsilon = \varepsilon_m = -n^2$ for $z > 0$ has components E_{x1} and E_{x2}, the continuity requirements for these tangential components gives $E_{x1} = E_{x2}$, resulting in following expression.

$$\frac{\partial H_{y1}}{\partial z} = -\frac{1}{n^2}\frac{\partial H_{y2}}{\partial z};\ \text{at } z = 0. \tag{15}$$

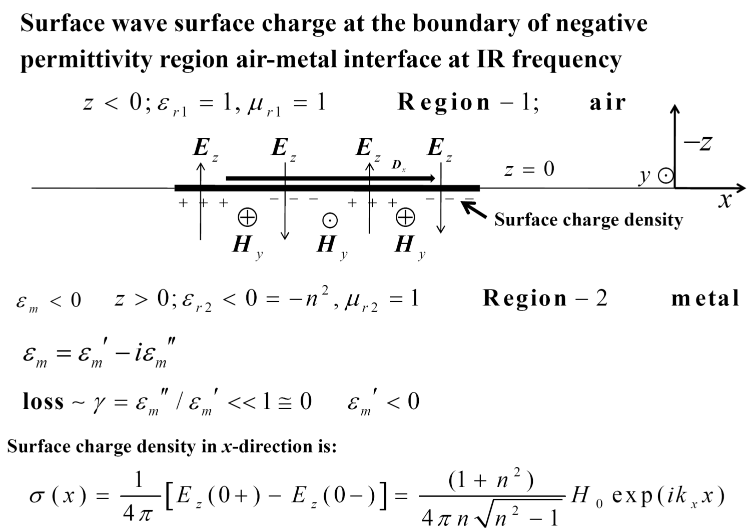

Figure 6. SPP Surface Wave Surface Change Density at Electric Resonance Condition.

For $n > 1$ this equation is satisfied and leads to a relation of wave of SPP and the refractive index for $\varepsilon_m < 0$ that is $k_{SPP} = k_x = (k_0 n)/\sqrt{n^2 - 1}$. Note for

$n > 1,$ the wave vector for SPP is real so that magnetic field H, decays exponentially in metal and free space. The component perpendicular to propagation of SPP the surface waves that is E_z, takes the following values at the interface $E_z(0-) = -(k_x/k_0)H_0 \exp(ik_x x)$ on the free space side $(z < 0)$; and $E_z(0+) = -(k_x/k_{z2})H_0 \exp(ik_x x) = (k_x/n^2 k_0)H_0 \exp(ik_x x) \neq E_z(0-)$ on the metal side $(z > 0)$. These are obtained from curl $H = -ik\varepsilon E$ at $z = 0^-$ and $z = 0^+$ sides. The discontinuity of the electric filed as seen the normal components $E_z(0^+) \neq E_z(0^-)$ manifests as surface change density $(\sigma(x))$, which propagates together with electric and magnetic field along the metal film surface

$$\sigma(x) = \frac{1}{4\pi}[E_z(0+) - E_z(0-)] = \frac{(1+n^2)}{4\pi n\sqrt{n^2-1}} H_0 \exp(ik_x x). \tag{16}$$

The surface wave which consists of EM field coupled to surface charge propagates by rearrangement of charge density, not surprising that its speed is always less than c, that is $c_x = \omega/k_x = c\sqrt{n^2-1}/n < c$; depicted in Figure 6.

When the refractive index has a property of approaching unity $-n^2 = \varepsilon_m \to -1$, the SPP speed approaches zero, the surface wave SPP stops on the surface. In this ideal case, the surface charge diverges (16), as $(n^2-1)^{-1/2}$ blows up; so does the normal component of Electric field-gives production of giant fields at electrostatic resonance.

In this section, we have justified that with permittivity value as negative, for infinite sheet will have resonances at its surface as surface charge density, which can be very high and thus its associated transverse electric field and are thus the ‘giant fields’. We can have any arbitrary shaped particle with negative permittivity that in the uniform elective field will have resonances giving surface charge density as well as associated giant fields. Now we generalize this above concept in concept in following section.

4. Generalization of Electrostatic Resonance Theory

Resonant behavior of dielectric object occurs at certain frequency for which object has dielectric permittivity negative value $\varepsilon < 0$, as described in previous sections, and also free space wavelengths of EM radiation is very large compared to the object dimensions. Say metal bead are embedded in dielectric substance will have effective negative permittivity and the plasma frequency will scale down from visible IR region (for metals) to microwave ranges. This is essence of creation of artificial structures of meta-material which behave as negative epsilon meta-material at the microwave region microwave region [1-10, 14, 19, 27, 29, 35, 38, 52, 53]. The free space wavelength of the EM radiation needs be very large compared to the dimensions of the object and its lattice dimensions, makes application effective medium theory possible [1-10, 14, 19, 27, 29, 35, 38], and from electrodynamics point of view quasi static [30] approximations are valid, this also suggests the resonance are electrostatic in nature [52] and [53], as they appear at specific negative values of dielectric permittivity for which source free electrostatic field may exist. Plausibly the electrostatic based resonance mechanism is explanation of illumination of the plasmoid. The idea of giant fields associated with resonances has been introduced in the earlier section, now we generalize the concept of electrostatic resonance.

We are interested in $\varepsilon < 0$ for which source free electrostatic field may exist. This source free field is curl free and divergence free inside volume of particle Γ^{+} and outside the volume of particle Γ^{-} of the dielectric object (nm sized particles ejected from solid substrate after application of near field of wave length about 12 cm for 2.45GHz), refer Figure 7. The potential is continuous across the boundary *S* of the object, while normal components of electric field follows (1), on the surface boundary *S*

$$\varepsilon E_n^{+} = \varepsilon_0 E_n^{-}. \tag{17}$$

The electric potential of the source free electric field can be represented as an electric potential of single layer of charge distribution over surface *S* [30], [52], [53].

$$V(P) = \frac{1}{4\pi\varepsilon_0} \int_s \frac{\sigma(Q)}{r_{QP}} dS_Q. \tag{18}$$

In other words, a single layer of electric charge (with surface charge density σ) on *S* creates the same electric field in the free space as soure free electric field may exist in presence of dielectric object [30, 52, 53]. It is apparent that electric field of the surface charge σ is curl free and divergence free in Γ^{-} and Γ^{+} regions, and potential is continuous across *S*. The normal component of Electric field of a single layer potential is given by [30, 39, 40, 52, 53].

We now simply assume that the particle in the Figure 7 is convex shaped (ellipsoid, spherical etc). There will be surface charge at the surface boundary, when the particle is placed in source free electric field. The surface charge and normal component of electric field for a flat surface and its resonance is described by expression (16). Thus our problem is to determine the Electric fields at point *P*, in Figure 7, normal to the surface. Let us first assume that the particle of Figure 7 is having surface charge density $\sigma(P)$ at point *P*, and at other points such as *Q*, the charge density is $\sigma(Q)$. In other words let this surface charge be the function of location of points at the surface *S*, for a very general case.

We can view the electric field at the point *P*, as electric field in an infinitesimal hole at *P* as sum of the fields from the rest of the shell plus the field due to an infinitesimal patch with surface charge density equal but opposite to patch cut-out. In other words remove a small patch at *P*, which then will have surface charge density opposite in sign that is $-\sigma(P)$. This patch is so small that we can consider as plane surface instead of curved surface; and the standard pill-box calculation applied for Gauss law for a surface of charge density $-\sigma(P)$ coulomb $/\,\mathrm{m}^2$ will give normal electric field from the surface as $-\sigma(\mathrm{P})/2\varepsilon_0$ [30, 52, 53].

Say the convex surface is a sphere of radius *R*, having charge of *q* coulombs, and let infinitesimal (circular) patch at *P* having very small radius of *a*, will have surface charge density $\sigma(P) = (q)/(4\pi R^2)\,\text{coulombs}/\mathrm{m}^2$. The total electric field at *P* is therefore is $E(P) = E_{\text{hole}} + E_{\text{spherical-shell}}$. The electric field of spherical shell by applying a Gauss surface just outside the shell is $E_{\text{spherical-shell}}(4\pi R^2) = q_{\text{enclosed}}/\varepsilon_0 = q/\varepsilon_0$; from here

$$E_{\text{spherical-shell}} = (q)/(4\pi\varepsilon_0 R^2).$$

From here we calculate $E(P) = \{-\sigma(P)/2\varepsilon_0\} + \{(q)/(4\pi\varepsilon_0 R^2)\} = (q)/(8\pi\varepsilon_0 R^2)$. If we were to calculate electric field at *P*, from inside the surface, the procedure is same but the field direction of the patch will be opposite to what we considered in above calculation. In the above calculation we assume that coulombs contents of the patch at P that is $q(a^2 / 4R^2)$ very small fraction of total charge q; and thus we have applied the Gauss law stating that total charge enclosed is q in spite of patch of radius a removed. Due to infinitesimal small patch we can have this assumption; and with all these arguments we write the electric field (normal to a surface S) at point P for just outside and just inside the surface of Figure 7 as (19); a general relation for an arbitrary shaped object, [30, 52, 53].

$$E_n^{\pm}(P) = \mp \frac{\sigma(P)}{2\varepsilon_0} + \frac{1}{4\pi\varepsilon_0} \int_s \sigma(Q) \frac{\mathbf{r}_{QP} \bullet \mathbf{n}_P}{r_{QP}^3} dS_Q. \tag{19}$$

By putting (19) into (17), and after following the steps, as described below we arrive at homogeneous boundary integral equation (20); written with kernel of integration $K(Q, P)$.

$$\varepsilon E_n^+ = \varepsilon_0 E_n^-,$$

$$-\varepsilon \frac{\sigma(P)}{2\varepsilon_0} + \varepsilon \frac{1}{4\pi\varepsilon_0} \int_s \sigma(Q) \frac{\mathbf{r}_{QP} \bullet \mathbf{n}_P}{r_{QP}^3} dS_Q$$

$$= +\varepsilon_0 \frac{\sigma(P)}{2\varepsilon_0} + \varepsilon_0 \frac{1}{4\pi\varepsilon_0} \int_s \sigma(Q) \frac{\mathbf{r}_{QP} \bullet \mathbf{n}_P}{r_{QP}^3} dS_Q,$$

$$-\varepsilon\sigma(P) + \varepsilon \frac{1}{2\pi} \int_s \sigma(Q) \frac{\mathbf{r}_{QP} \bullet \mathbf{n}_P}{r_{QP}^3} dS_Q$$

$$= +\varepsilon_0\sigma(P) + \varepsilon_0 \frac{1}{2\pi} \int_s \sigma(Q) \frac{\mathbf{r}_{QP} \bullet \mathbf{n}_P}{r_{QP}^3} dS_Q,$$

$$\varepsilon\sigma(P) + \varepsilon_0\sigma(P) = \varepsilon \frac{1}{2\pi} \int_s \sigma(Q) \frac{\mathbf{r}_{QP} \bullet \mathbf{n}_P}{r_{QP}^3} dS_Q - \varepsilon_0 \frac{1}{2\pi} \int_s \sigma(Q) \frac{\mathbf{r}_{QP} \bullet \mathbf{n}_P}{r_{QP}^3} dS_Q,$$

$$\sigma(P) = \left(\frac{\varepsilon - \varepsilon_0}{\varepsilon + \varepsilon_0}\right) \frac{1}{2\pi} \int_s \sigma(Q) \frac{\mathbf{r}_{QP} \bullet \mathbf{n}_P}{r_{QP}^3} dS_Q.$$

From above derivation we write the following in compact integral form, that is

$$\sigma(P) = \frac{\lambda_{\text{eigen}}}{2\pi} \int_S K(Q, P) dS_Q, \tag{20}$$

where the kernel in integral equation of (20) is

$$K(Q,\ P) = \frac{\mathbf{r}_{QP} \bullet \mathbf{n}_P}{r_{QP}^3}. \tag{21}$$

The eigen-value is [52, 53]

$$\lambda_{\text{eigen}} = \frac{\varepsilon - \varepsilon_0}{\varepsilon + \varepsilon_0} \tag{22}$$

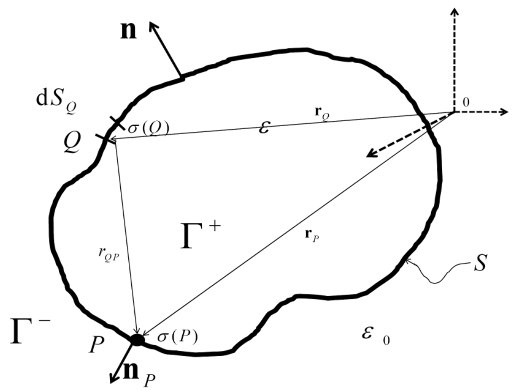

Figure 7. The dielectric particle in curl free divergence free Electric field.

From (22), we will have negative ε as $\varepsilon = -\varepsilon_0(\lambda_{\text{eigen}} + 1)/(\lambda_{\text{eigen}} - 1)$, for particular shape of *S*. The (20) is Fredholm's homogeneous integral equation (of second kind) which has from [52, 53]

$$f(x) = \lambda_f \int_a^b K(x,\ y) f(y) dy. \tag{23}$$

The source free electric fields may exist only for such values of ε, that (20) has non zero solutions. In other words resonant values of ε (and corresponding resonant frequencies) as well as resonant electrostatic modes are embedded in eigen-values and eigen-function of (20), which should be found. It is shown in [41, 42, 52, 53] the interesting properties of the eigen-values. First, all the eigen-values λ_{eigen} are real, with $\lambda_{\text{eigen}} = 1$ as eigen-value; this value corresponds to a case that $\varepsilon \to \infty$; and its respective eigen-function $\sigma(P)$ is distribution of surface charge of a conductor surface (this value is not required for our case). All other eigen-value except unity, corresponds to a source free is resonance configuration of electric field and according to (22) these configuration may exists only for negative values of ε. After the negative values of ε are found through (20), the approximate frequency dependency of ε (say Drude model [1-10, 14, 19, 27, 29, 35, 38]) can be get employed to find resonant frequencies, that is $\varepsilon = \varepsilon_0(1-(\omega_p^2/\omega^2))$; for $\omega < \omega_p$, we get negative dielectric permittivity, where ω_p is the plasma frequency.

5. Discussion on Electrostatic Resonance and its Properties

It is apparent that mathematical structure of the integral in (20) is invariant with respect to scaling *S* [52, 53]. This leads to unique property of electrostatic resonance, that is, 'the resonant frequency depends on object shape but are scale invariant with respect to object dimension, provided they remain well below the free space wave length of excitation EM radiation'.

If $\mathbf{E}_i$ and $\mathbf{E}_k$ are the electric fields corresponding to eigen-functions σ_i and σ_k, then [39, 52, 53] the fields are orthogonal, that is

$$\int_{\Gamma^{\pm}} \mathbf{E}_i \bullet \mathbf{E}_k d\Gamma = 0. \tag{24}$$

The orthogonality (24) holds separately for Γ^+ and Γ^- regions. However, the eigen-functions $\sigma_1(Q)$ and $\sigma_2(Q)$ corresponding to eigen-values $\lambda_{\text{eigen}-1}$, $\lambda_{\text{eigen}-2}$ are not orthogonal on *S*, because the kernel (21) of the integration (20) is not symmetric (non Hermitian) [39, 52, 53].

These orthogonality conditions can be useful in analysis of the coupling of the specific resonance mode to the incident electric field. For example we take spherical shaped particle in Figure 7; its resonance modes will be different from ellipsoid (elliptical-harmonics). However, there are resonant modes with uniform electric field in Γ^+. This means according to orthogonality, condition that only these uniform resonant modes will be excited by uniform (within Γ^+) incident radiation. The condition of uniformity with in Γ^+ of the incident radiation is some extent natural due to object dimensions smaller to free space radiation as we stressed earlier. For complex shaped objects many resonant modes with appreciable average value of electric field components over Γ^{+} may exist. All such modes will be well coupled to the uniform incident radiation and can be excited by such incident fields at respective frequency of resonance.

For a convex S of Figure 7 estimate of eigen-values can be derived via estimate [40, 52, 53];

$$\left|\lambda_{\text{eigen}}\right| > C = \frac{1}{1 - \frac{A}{4\pi Rd}}, \tag{25}$$

where A is area of S; R is maximum radius of curvature of S; d the diameter of Γ^{+}. Using (25) and (22), the upper bound and lower bound for possible resonance values of permittivity ε can be obtained as

$$\frac{1+C}{1-C} < \frac{\varepsilon}{\varepsilon_0} < \frac{1-C}{1+C}. \tag{26}$$

For plasma, we have dispersion of permittivity as Drude model; that is, $(\varepsilon/\varepsilon_0) = 1 - (\omega_p^2/\omega^2)$, [1-10, 14, 19, 27, 29, 35, 38] substituting into (26) we have

$$\frac{C-1}{2C} < \frac{\omega^2}{\omega_P^2} < \frac{C+1}{2C}, \tag{27}$$

which says that bandwidth for resonance frequency is smaller than $\omega_p/\sqrt{C} = \omega_p\sqrt{1-(A/2Rd)}$, also in [52, 53].

For a unit sphere the surface charge density will be given by spherical harmonics. The standard eigen function for spherical harmonics is given by [30, 52, 53] $Y_{l,m}(\theta, \varphi)$. This spherical harmonics eigen function is defined in terms of Legendre's polynomial, $P_{l,m}(x)$ as $Y_{l,m}(\theta, \varphi) = P_{l,m}(\cos\theta)e^{im\varphi}$, where $-l \le m \le +l$, θ and φ are co-altitude polar $(0 \le \theta \le \pi;$ North pole to South pole) angle and longitude azimuth angle $(0 \le \varphi \le 2\pi)$ of spherical coordinates respectively; with corresponding eigen values $\lambda_{\text{eigen}-l} = 2l+1$. From (22) giving ε as $\varepsilon_l = -\varepsilon_0(1 + 1/l)$; and valid for, $l \ge 1$. The lowest electrostatic resonant mode, for $l = 1$ is $\varepsilon_1 = -2\varepsilon_0$ is uniform in Γ^{+}, and only can be excited (into three possible spherical harmonic mode) by uniform incident radiation, that is for $l = 1$, we have three spherical harmonics with $m \in \{-1, 0, 1\}$, giving $Y_{1,0}(\theta, \varphi)$, $Y_{1,1}(\theta, \varphi)$. and $Y_{1,-1}(\theta, \varphi)$. The first spherical harmonics, with $m = 0$ represents 'zonal mode', where the charge positive and negative are distributed by equatorial symmetry. The north and south poles getting maximum positive charge density and negative charge density. The mode with $m = \pm 1$ are 'sectorial modes' and symmetric with respect to z-axis, where the charge distribution is spread in two sectors eastern and western. The 'tesseral mode' is not existing with $l = 1$ and $m = \pm 1$. Thus there exist resonant modes with permittivity value as negative, where the charge density and correspondingly electric field will be very large, at resonant frequencies, for arbitrary shaped particles ejecting out from solid substrate of our experiment.

We saw via several ways that 'Epsilon Negative' condition is criteria for obtaining electrostatic resonance and giant local electric field manifestations. As a special case $\varepsilon_1 = -2\varepsilon_0$, is for case of spherical geometry in Figure 7. We get the same condition by classical Maxwell-Garnet Theory and application of Clausius-Mossotti relation; for a spherical dielectric inclusion in a dielectric host medium. Say, instead of free space the material particles with ε_1, if embedded in a host with dielectric permittivity ε_h, then the condition of Plasmon resonance would be $\varepsilon_1 = -2\varepsilon_h$; which we will derive again classically via concept of polarizability, and Lorentz sphere, and Lorentz local field expression [54-56].

Without loss of generality, consider a dense optical medium, molecular dipoles arranged in cubic lattice. It was pointed out first by Lorentz, that the local field experienced by a molecule, is 'not' the macroscopically averaged field E, but a local field called E_L (L implies local) . This is fact, as there are indeed giant fields inside an atom or within the gaps between atoms in solids, because all solids are shown to be non-uniform when examined at atomic scale. However, all these local fluctuations are averaged out to zero if you look at the material at a much larger scale than that of atomic features. Macroscopically, thus the magnitude of the field in a homogeneous medium is regarded as constant if loss is not an issue. However, when we study the effect of an external field upon an individual atom or molecule or particle, the local features of EM fields must be carefully analyzed.

To evaluate the local field E_L at the site of say molecule in a uniform solid, the molecule is 'imagined' to be surrounded by a spherical cavity (called Lorentz sphere), Figure 8. The radius R of the sphere is macroscopically small in order to accommodate the discrete nature of the medium very close to the molecule, but it is microscopically large enough so that the matrix just outside be treated as continuous medium. The space inside the sphere is free space with dielectric constant ε_0, that of vacuum, because the gap between the individual molecules contains nothing but free-space. When the external electric field is applied, electric charges are distributed around the surface of (hypothetical) Lorentz sphere, which gives rise to additional field imposed upon the central molecule, refer Figure 8.

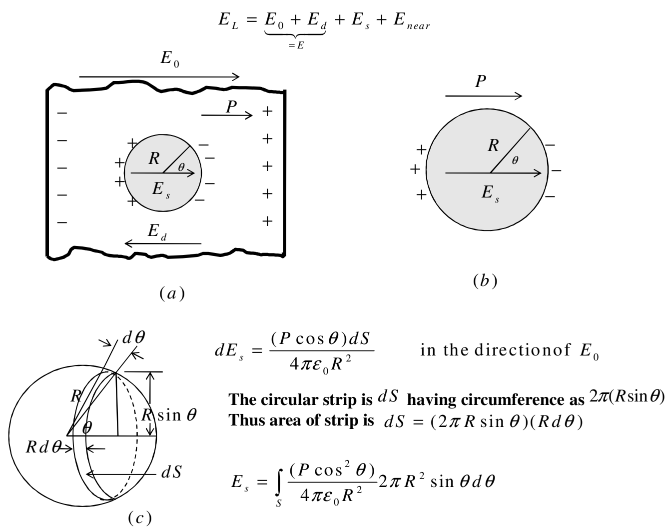

Figure 8. Lorentz sphere for calculating local electric field.

The local field acting on the central dipole can be decomposed as sum of four components:

$$E_L = E_0 + E_d + E_s + E_{\text{near}}, \tag{28}$$

where E_0 is the external field; E_d, the depolarization field, is due to the polarization charges lying at external surface of medium; P, the macroscopic (volume) polarization is equal related to depolarization field as $E_d = -P/\varepsilon_0$; E_s denotes the field due to polarization charges lying on surface of Lorentz sphere; E_{near} is the field induced by other charges lying within the sphere.

The term $E_0 + E_d$ in expression (28) is the homogeneous field averaged over the entire volume of the material. It exactly the macroscopic field E, that enters the Maxwell's equation, and has constant magnitude throughout the medium for a homogeneous medium. On the other hand the local field E_L is the microscopic field that fluctuates rapidly within the medium, and that can be giant like, at the molecular sites. Refer Figure 8a for the fields.

We need to calculate E_s. We relate surface charge density on the surface of Lorentz sphere to the polarization P in the medium, to evaluate E_s. That is total charge over a surface segment dS is $(P\cos\theta)dS$, where θ is the angle between P and the normal of the surface segment, Figure 8b. This amount of surface charge produces an electric field dE_s, at a distance R (in radial direction), given by

$$dE_s = \frac{(P\cos\theta)dS}{4\pi\varepsilon_0 R^2}. \tag{29}$$

The total field E_s resulting from all the surface charges on the Lorentz sphere is directed along the external field E_0, with a magnitude (horizontal component) as in Figure 8b.

$$E_s = \int_s \frac{(P\cos\theta)dS}{4\pi\varepsilon_0 R^2}\cos\theta = \int_s \frac{(P\cos^2\theta)}{4\pi\varepsilon_0 R^2}dS. \tag{30}$$

The circular strip is dS having circumference as $2\pi(R\sin\theta)$. Thus area of strip is $dS = (2\pi R\sin\theta)(Rd\theta)$, refer Figure 8c.

$$E_s = \int_s \frac{(P\cos^2\theta)}{4\pi\varepsilon_0 R^2}2\pi R^2\sin\theta d\theta. \tag{31}$$

We do the following steps for evaluating (31)

$$E_s = \int_s \frac{(P\cos^2\theta)}{4\pi\varepsilon_0 R^2}2\pi R^2\sin\theta d\theta = \int_{\theta=0}^{\theta=\pi} \frac{(P\cos^2\theta)}{4\pi\varepsilon_0 R^2}2\pi R^2\sin\theta d\theta$$

$$= \frac{P}{2\varepsilon_0}\int_0^{\pi}\cos^2\theta\sin\theta d\theta,$$

$$u = \cos\theta, \quad du = -\sin\theta d\theta, \quad E_s = -\frac{P}{2\varepsilon_0}\int_1^{-1} u^2 du,$$

$$E_s = -\frac{P}{2\varepsilon_0}\left[\frac{u^3}{3}\right]_1^{-1} = -\left(\frac{P}{2\varepsilon_0}\right)\left[\frac{-1}{3} - \frac{1}{3}\right] = \frac{P}{3\varepsilon_0}.$$

Therefore

$$E_L = E_0 + E_d + E_s + E_{\text{near}} = E + E_s = E + \frac{P}{3\varepsilon_0}, \quad \text{with } E_{\text{near}} = 0. \tag{32}$$

We assumed E_{near}, the field due to dipoles within the spherical cavity to be zero. Actually this field depends upon the crystal structure, in liquids or gases it vanishes, where the dipoles are randomly distributed in uncorrelated positions. In this example of solid in our case, we assumed a cubic crystal lattice, where E_{near} vanishes owing to the lattice symmetry. The expression for total local Lorentz field is

$$E_L = E + \frac{P}{3\varepsilon_0}. \tag{33}$$

The field acting at an atom/molecule/particle site is macroscopic field E plus $P/3\varepsilon_0$, from polarization of other atoms/molecules/particles in the system: this is Lorentz relation.

We relate polarization P to the electric dipole moment of each atom/molecule/particle. Denote α as polarizability of one atom/molecule/particle; if N denotes volume density of these atom/molecule/particle dipoles then

$$P = N\alpha E_L = N\alpha\left(E + \frac{P}{3\varepsilon_0}\right) \text{ gives } \frac{N\alpha}{3\varepsilon_0}P = P - N\alpha E. \tag{34}$$

We also have constitutive relation of displacement vector to the electric field and volumetric polarization, (in frequency domain) as

$$D = \varepsilon_0 E + P = \varepsilon_0(1 + \chi_e)E = \varepsilon_0\varepsilon_r E. \tag{35}$$

Use from this (35) by dropping subscript r; the expression $P = \varepsilon_0(\varepsilon - 1)E$ and via following steps we obtain the polarizability α

$$\frac{N\alpha}{3\varepsilon_0}P = P - N\alpha E,$$

$$\frac{N\alpha}{3\varepsilon_0}\varepsilon_0(\varepsilon - 1)E = \varepsilon_0(\varepsilon - 1)E - N\alpha E,$$

$$\frac{N\alpha}{3}(\varepsilon - 1) + N\alpha = \varepsilon_0(\varepsilon - 1),$$

$$\frac{N\alpha}{3}[(\varepsilon - 1) + 3] = \varepsilon_0(\varepsilon - 1),$$

$$\frac{N\alpha}{3\varepsilon_0} = \frac{\varepsilon - 1}{\varepsilon + 2},$$

$$\alpha = \frac{3\varepsilon_0}{N}\frac{(\varepsilon - 1)}{(\varepsilon + 2)}.$$

This is Clausius-Mossotti relation, which gives the necessary link between the macroscopic observable and the microscopic parameter α. The Claussius-Mossotti relation relating the macroscopic observables to microscopic parameter is not mysterious, because there is a distinct connection between the electric response of individual molecule and the macroscopic behavior of the bulk material described by dielectric function (susceptibility). We assume the spherical particles of relative dielectric permittivity ε_1 are embedded in the host medium of relative permittivity as ε_h, and we re-write the Clausius-Mossotti relation as

$$\frac{N\alpha}{3\varepsilon_0} = \frac{\varepsilon - 1}{\varepsilon + 2} \text{ becomes } \frac{N\alpha}{3\varepsilon_0\varepsilon_h} = \frac{\varepsilon - \varepsilon_h}{\varepsilon + 2\varepsilon_h} \text{ or } \alpha = \frac{3\varepsilon_0\varepsilon_h}{N}\left(\frac{\varepsilon - \varepsilon_h}{\varepsilon + 2\varepsilon_h}\right). \tag{36}$$

In above, ε represents the effective permittivity of the composite. Note that $(1/N)$ is volume occupied by each molecule in above relation. If f is the filling fraction of the material in the host, i.e., with ε_1, then we can rewrite above as

$$\alpha = \frac{3\varepsilon_0\varepsilon_h f}{N}\left(\frac{\varepsilon_1 - \varepsilon_h}{\varepsilon_1 + 2\varepsilon_h}\right). \tag{37}$$

We substitute (37) in (36) for α and get the following

$$\frac{\varepsilon - \varepsilon_h}{\varepsilon + 2\varepsilon_h} = f\left(\frac{\varepsilon_1 - \varepsilon_h}{\varepsilon_1 + 2\varepsilon_h}\right). \tag{38}$$

This is Maxwell-Garnet Theory MGT for Effective Medium approximation. We do the following arithmetic to obtain another form of (38) as indicated below.

$$\frac{\varepsilon - \varepsilon_h}{\varepsilon + 2\varepsilon_h}\, f\,\frac{\varepsilon_1 - \varepsilon_h}{\varepsilon_1 + 2\varepsilon_h} = fx, \text{ where } x = \frac{\varepsilon_1 - \varepsilon_h}{\varepsilon_1 + 2\varepsilon_h},$$

$$\varepsilon - \varepsilon_h = \varepsilon f x + 2\varepsilon_h f x, \quad \varepsilon(1 - fx) = \varepsilon_h(1 + 2fx),$$

$$\varepsilon = \varepsilon_h \frac{1 + 2fx}{1 - fx} = \varepsilon_h \frac{1 + 2f \dfrac{\varepsilon_1 - \varepsilon_h}{\varepsilon_1 + 2\varepsilon_h}}{1 - f \dfrac{\varepsilon_1 - \varepsilon_h}{\varepsilon_1 + 2\varepsilon_h}}. \tag{39}$$

This is known as Maxwell-Garnet formula, describing the 'bulk' effective permittivity of a composite in terms of the permittivity of inclusion ε_1 and the host dielectric ε_h. For metal-dielectric, we can view the metal as the inclusion while the dielectric component serves as host.

Although the effective permittivity in MGT can reach the permittivity of the two constituents when the f approaches the two extremes $f = 0$ and $f = 1$, giving $\varepsilon = \varepsilon_h$, $\varepsilon = \varepsilon_1$, the MGT formula shows that MGT treats the matrix and the inclusion in unsymmetrical fashion. Therefore before evaluating the ε of the two-phase composites, one component should be treated as host and the other one as inclusion. This asymmetry is particularly strong when the difference in the permittivity of the two is large. In fact the MGT gives reasonable estimation of effective ε only when the volume filling fraction f of the inclusion is much smaller than unity and that is exactly in our case of plasmoid.

Approximation to Maxwell-Garnet formula by following steps we get

$$x = \frac{\varepsilon_1 - \varepsilon_h}{\varepsilon_1 + 2\varepsilon_h}, \quad \varepsilon = \varepsilon_h \frac{1 + 2fx}{1 - fx}, \quad f << 1,$$

$$\varepsilon = \varepsilon_h (1 + 2fx)(1 - fx)^{-1} \cong \varepsilon_h (1 + 2fx)(1 + fx) = \varepsilon_h [1 + 3fx + \mathcal{O}(f^2 x^2)],$$

$$\varepsilon = \varepsilon_h + 3f\varepsilon_h \frac{\varepsilon_1 - \varepsilon_h}{\varepsilon_1 + 2\varepsilon_h} + \mathcal{O}(f^2). \tag{40}$$

The resonance is occurring at $\varepsilon_1 = -2\varepsilon_h$ which represents surface plasmon resonance of an isolated metal spherical inclusion embedded in the host dielectric. From the Drude model for noble metal $\varepsilon_1 = \varepsilon_m = 1 - \omega_p^2 / \omega^2 = -2\varepsilon_h$; gives $\omega = \omega_p / \sqrt{1 + 2\varepsilon_h}$; as the surface plasmon resonance frequency. We derived this condition earlier too.

6. Conclusion

The discussion in this paper gives a plausible explanation to observation of lit plasmoid; via classical electrodynamics principles. The dielectric permittivity of the particulates ejecting out from molten solid substrate having negative values at the resonances is what causes giant surface densities accompanied by giant surface electric fields; after its interaction with the existing EM radiation. These giant fields cause local discharges, thereby glowing the entire plasmoid volume; as long as the EM field remains.

Acknowledgement

This work is supported fully by Board of Research in Nuclear Science (BRNS), Department of Atomic Energy (DAE). The project is called "Material Joining and Drilling with Microwave."

References

[1] V. G. Veselago, Electrodynamics of materials with negative index of refraction, Physicsâ Uspekhi 46(7) (2003), 764-768.

[2] Shantanu Das, Review on composite negative refractive indexed material with left handed Maxwell systems, Fundamental Journal of Modern Physics 3(1) (2012), 13-89.

[3] V. G. Veselago, The electrodynamics of substances with simultaneously negative values of ε and μ, Soviet Physics Uspekhi 10(4) (1968), 509-514.

[4] V. Veselago, L. Braginsky, V. Shklover and C. Hafner, Negative refractive index materials, J. Comput. Theor. Nanosci. 3 (2006), 1-30.

[5] J. B. Pendry, A. L. Holden, D. J. Robbins and W. J. Stewart, Magnetism from conductors and enhanced non-linear phenomena, IEEE Trans. on Microwave Theory and Techniques 47(11) (1999), 2075-2084.

[6] J. B. Pendry, Time reversal and negative refraction, Science 322 (2008), 71-73.

[7] J. B. Pendry, J. Holden, W. J. Stewart and I. Youngs, Extremely low frequency plasmons in metallic mesostructures, Phys. Rev. Lett. 76(25) (1996), 4773-4776.

[8] J. B. Pendry, J. Holden, D. J. Robbins and W. J. Stewart, Low frequency plasmons in thin wire structures structures, J. Physics: Condensed Matter 10 (1998), 4785-4808.

[9] Amitesh Kumar, Arijit Mazumder, Subal Kar and Shantanu Das, Possibilities of left handed maxwell systems (metamaterials) application in laser, nano-technology and

sub-wavelength imaging for medical diagnostic, Synergy in Physics & Industry, BARC (SPI-January 2013).

[10] J. B. Pendry, Negative refraction makes a perfect lens, Phys. Rev. Lett. 85(18) (2000), 3966-3969.

[11] H. Minkowski, Die Graddgleichugen fur die elektromagnetischen Vorgange in bewegten Korpem, Nachr. Ges. Wiss. Gottingen. Math. Phys. K1 53-111 Nachr. 1908.

[12] Abraham, Zur Electrodynamik bewegten Korpen, Rend. Circ. Matem. Palermo (1909), 1-28.

[13] P. W. Milonni, Field quantization and radiative processes in dispersive dielectric media, J. Modern Optics 42, 1995.

[14] Shantanu Das, Lectures: Parts 1-8 Left Handed Maxwell Systems (Google search), class room lectures for the reversed electrodynamics, 2010.

[15] Shantanu Das, Saugata Chaterjee, Amitesh Kumar, Paulami Sarkar, Arijit Majumder, Anant Lal Das and Subal Kar, A new look at the nature of linear momentum and energy inside Negative Refractive Media, Physica Scripta 84 (2011), 0357078.

[16] Shantanu Das, Saugata Chaterjee, Amitesh Kumar, Paulami Sarkar, Arijit Majumder, Ananta Lal Das and Subal Kar, A new mechanics of corpuscular wave transport of momentum and energy inside negative refractive media, Fundamental J. Modern Physics 1(2) (2011), 223-246.

[17] Shantanu Das, Quantized energy momentum and wave for an electromagnetic pulse - A single photon inside negative refractive media, J. Modern Physics 2(12) (2011), 1507-1522.

[18] Souagata Chatterjee, Amitesh Kumar, Arijit Mazumder, Paulami Sarkar, Subal Kar and Shantanu Das, Particle energy momentum transport for negative refractive index material (NRM) - anomalous concepts, ISAP 2011- Korea Conference 2011.

[19] Amitesh Kumar, Arijit Majumder, Sougata Chaterjee, Subal Kar and Shantanu Das, A novel approach to determine the plasma frequency for wire media, Metamaterials 6 (2012), 43-50.

[20] Sougata Chaterjee, Amitesh Kumar, Paulami Sarker, Arijit Mazumder, Subal Kar and Shantanu Das, A comparative study on different magnetic inclusion structures with analytical modelling and simulation studies, Int. Symposium on Antennas and Propagation, Korea ISAP-2011.

[21] Amitesh Kumar, Arijit Mazumder, Sougata Chaterjee, Subal Kar and Shantanu Das, Generalized approach to determine plasma frequency for wire medium: useful for meta-material applications, Conference AEMC-Kolkata, 2011.

[22] A. Kamli et. al., Coherent control of low loss surface polaritons, Phys. Rev. Lett. 101 (2008), 263601.

[23] H. Kogelnik, Theory of Optical-waveguides in Guided Wave Optoelectronics, T. Tamer, ed., Springer-Verlag, Berlin, 1988, pp. 7-88.

[24] A. Anatoly, Barybin and A. Victor, Dmitriev, Modern electrodynamics and coupled-mode theory: application to guided-wave optics, Rinton Press, Princeton, N. J., 2002.

[25] U. Leonhardt, Momentum in an uncertain light, Nature 444 (2006), 823-824.

[26] Robert N. Pfeifer, Timo A. Nieminen, Norman R. Heckenberg and Halina Rubinsztein-Dunlop, Momentum of an electromagnetic wave in dielectric media, Rev. Mod. Phys. 79 (2007), 1197.

[27] D. R. Smith, W. J. Padilla, D. C. Vier, S. C. Nemat Nasser and S. Schultz, Composite medium with simultaneously negative permeability and permittivity, Phys. Rev. Lett. 84(18) (2000), 4184-4187.

[28] D. R. Smith and N. Kroll, Negative refractive index in left handed materials, Phys. Rev. Lett. 85(14) (2000), 2933-2936.

[29] D. R. Smith, S. Schultz, P. Markoš and C. M. Soukoulis, Determination of effective permittivity and permeability of metamaterials from reflection and transmission coefficients, Phys. Rev. B 65 (2002), 195104.

[30] J. D. Jackson, Classical Electrodynamics, 3rd ed., Willey, New-York, 1999.

[31] R. W. Ziolkowski and E. Heyman, Wave propagation in media, having negative permittivity and permeability, Phys. Rev. E 64 (2001), 056625.

[32] R. Shelby, D. R. Smith and S. Schultz, Expermental verification of a negative index of refraction, Science 292 (2001), 77-79.

[33] V. Lindell, S. Tretyakov, K. I. Nikoskinen and S. Ivonen, BW media with negative parameters, capable of supporting backward waves, Microwave and Optical Tech. Letters 31(2) (2001), 129-133.

[34] A. Grbic and G. V. Eleftheriades, Experimental verification of backward wave radiation from a negative refractive index metamaterial, J. Appl. Phys. 92(1) (2002), 5930-5935.

[35] S. Anantha Ramakrisna, Physics of negative refractive indexed materials, Rep. Phys. 68 (2005), 449-521.

[36] Sandi Setiawan, Tom G. Mackay and Akhilesh Lakhtak, A comparison of super radiance and negative phase velocity phenomena in ergosphere of rotating black hole, Phys. Lett. A 341 (2005), 15-21.

[37] Roman Kolesov et al., Wave-particle duality of single surface plasmon polariton, Nature Physics 5 (2009), 470-474.

[38] Shantanu Das, Electromagnetic energy ad momentum inside negative refractive

indexed material - a new look at concept of photon, 99th Indian Science Congress, Bhubaneswar, India, 2012.

[39] O. D. Kellog, Foundation of Potential Theory, McGraw Hills, New-York, 1929.

[40] S. G. Mikhlin, Mathematical Physics and Advanced Course, Amsterdam, North-Holland, 1970.

[41] N. M. Gunter, Die Potential theorie und ihre Amwendungen anf Grundaufgoben der Mathematischen Physik, Teubner Verlag, Leipzig, 1947.

[42] D. Colton and R. Kres, Integral Equations Method in Scattering Theory, John Willey & Sons, New York, 1983.

[43] Titto John George, Apurbba Kumar Sharma and Pradeep Kumar, A feasibility study on microwave drilling of metallic materials, i-manager's J. Mechanical Engineering (JME) 2(2) (2012), 1-7.

[44] Shantanu Das and Apurba Kumar Sharma, Microwave drilling of materials, BARC News letter, Issue No. 329, Nov.-Dec. 2012.

[45] A. I. Al-Shamma, S. R. Wylie, J. Lucas and R. A Stuart, Microwave plasma jet for material processing at 2.45 GHz, J. Materials Processing Technology 121 (2002) 143-147.

[46] J. B. A. Mitchell, J. L. LeGarrec, M. Sztucki, T. Narayanan, V. Dikhtyar and E. Jerby, Evidence for nanoparticles in microwave-generated fireballs observed by synchrotron X-ray scattering, Phys. Rev. Lett. 100(6) (2008), 065001.

[47] Vladimir Dikhtyar and Eli Jerby, Fireball ejection from a molten hot spot to air by localized microwaves, Phys. Rev. Lett. 96 (2006), 045002.

[48] E. Jerby, A. Golts, Y. Shamir, V. Dikhtyar, J.B.A. Mitchell, J. L. LeGarrec, T. Narayanan, M. Sztucki, N. Eliaz, D. Ashkenazi and Z. Barkay, Fireballs ejected from solids and liquids by localized microwaves, Proceedings Global Congress on Microwave Energy Applications (GCMEA-1), Otsu, Japan, August 4-8, 2008.

[49] E. Jerby, A. Golts, Y. Shamir, S. Wonde, J. B. A. Mitchell, J. L. LeGarrec, T. Narayanan, M. Sztucki, D. Ashkenazi,1 Z. Barkay and N. Eliaz, Nanoparticle plasma ejected directly from solid copper by localized Microwaves, Appl. Phys. Lett. 95 (2009), 191501.

[50] E. Jerby, V. Dikhtyar, O. Aktushev and U. Grosglick, The microwave drill, Science 298 (2002), 587-589.

[51] E. Jerby, O. Aktushev and V. Dikhtyar, Theoretical analysis of the microwave-drill near-field localized heating effect, J. Appl. Phys. 97 (2004), 034909.

[52] Abdelilah Mejdoubi and Christian Brosean, Electrostatic resonance of clusters of dielectric cylinders, a finite element simulation, Phys. Lett. A 372 (2008), 741-748.

[53] D. R. Fredkin and I. D. Mayergoyz, Resonant behavior of dielectric objects (Electrostatic resonances), Phys. Rev. Lett. 91(25) (2003).

[54] R. Landauer, Electrical conductivity in inhomogeneous media, J. C. Garland and D. B. Tanner, eds., AIP Conference Proceedings, New York, 1977, pp. 2-45.

[55] A. Ishimaru, Wave Propagation and Scattering in Random Media, Academic, New York, 1978.

[56] V. M. Shalaev, Non-linear Optics of Random Media: Fractal Composites and Metal-dielectric Films, Springer-Berlin, 2000.

[57] Wenshan Cai and Vladimir Shalaev, Optical Meta-materials Fundamentals and Applications , Springer, New York, 2010.